Contribution from the Department of Chemistry and Laboratory for Molecular Structure and Bonding, Texas A&M University, College Station, Texas 77843, and Department of Chemistry, University of New Orleans, New Orleans, Louisiana 70148

Oxidative Addition to M–M Quadruple Bonds. Preparation of New Edge-Sharing Bioctahedral Complexes of the Type $(L\text{-}L)Cl_2M(\mu\text{-}Cl)_2MCl_2(L\text{-}L)$ (M = Mo, W, L-L = 1,2-Bis(diphenylphosphino)ethane; M = Mo, L-L = 1-(Diethylphosphino)-2-(diphenylphosphino)ethane)

P. A. Agaskar,[1a] F. A. Cotton,*[1a] K. R. Dunbar,[1a] L. R. Falvello,[1a] and C. J. O'Connor[1b]

Received May 19, 1987

The reaction of chlorine with the quadruply bonded compounds $M_2Cl_4(dppe)_2$ (dppe = $Ph_2PCH_2CH_2PPh_2$) affords the oxidized products $M_2(\mu\text{-}Cl)_2Cl_4(dppe)_2$ (M = Mo, W). A third compound $Mo_2(\mu\text{-}Cl)_2Cl_4(dedppe)_2$ (dedppe = $Et_2PCH_2CH_2PPh_2$) was isolated from the reaction of $Mo_2Cl_4(dedppe)_2$ with dichloromethane. The air-stable M_2^{6+} complexes were characterized by elemental analysis, IR spectroscopy, and X-ray crystallography. Crystals of $Mo_2Cl_6(dppe)_2 \cdot 4CH_2Cl_2$ (**1**) are monoclinic, space group $C2/m$, with a = 17.288 (2) Å, b = 18.500 (2) Å, c = 13.855 (4) Å, β = 121.14 (2)°, V = 3793 (3) Å^3, and Z = 2. The structure was refined to R = 0.0694 (R_w = 0.0718), and quality of fit = 2.21. The molecule has crystallographic $2/m$ (C_{2h}) symmetry; the virtual symmetry of the core is D_{2h}. The Mo–Mo distance is 2.762 (1) Å. $Mo_2Cl_6(dedppe)_2 \cdot 2CH_2Cl_2$ (**2**) crystallizes in the monoclinic system, space group $P2_1/c$ with the following unit cell dimensions: a = 12.148 (6) Å, b = 10.707 (5) Å, c = 22.529 (5) Å, β = 101.57 (4)°, V = 2870 (4) Å^3, Z = 2. The binuclear Mo_2 unit resides on a crystallographic inversion center. Final residuals for the structure are R = 0.064 (R_w = 0.079); goodness of fit = 1.56. The Mo–Mo distance is 2.785 (3) Å, which is very similar to the distance in **1**. The ditungsten complex $W_2Cl_6(dppe)_2 \cdot 4CH_2Cl_2$ (**3**) crystallizes in the triclinic system, space group $P\bar{1}$, with a = 12.521 (2) Å, b = 13.956 (3) Å, c = 20.690 (5) Å, α = 104.36 (4)°, β = 92.34 (3)°, γ = 112.34 (4)°, V = 3202 (4) Å^3, and Z = 2. The asymmetric unit is defined by two independent molecules of $W_2Cl_6(dppe)_2$, each of which resides on an inversion center, and four molecules of CH_2Cl_2 that occupy general positions. The two ditungsten molecules are structurally alike, and their corresponding bond distances and angles are very similar. The average W–W distance is 2.681 [1] Å. Successful refinement gave R = 0.0441 (R_w = 0.0538). In all three cases, the molecules possess an edge-sharing bioctahedral geometry in which the metals are bridged by two Cl atoms. Two bidentate phosphine ligands assume a chelating mode in the equatorial plane, which is defined by the metal and μ-Cl atoms; above and below the equatorial plane are apical positions occupied by terminal chloride ligands. Compounds **1** and **3** have been characterized magnetically, and **1** has been further studied by cyclic voltammetry and UV–visible spectroscopy.

Introduction

Binuclear complexes possessing unsaturated M–M bonds undergo oxidative-addition reactions with a variety of substrates. Recent work in these laboratories has demonstrated the general nature of oxidative addition chemistry for double,[2] triple,[3-5] and quadruple[6] bonds. Our primary interest in these reactions is their use as high-yield synthetic routes for the preparation of specific M_2L_{10} compounds that have been targeted for X-ray studies.

Several years ago we reported that novel dimolybdenum(III) complexes with bridging SR^- groups can be prepared by oxidative addition of RSSR to Mo–Mo quadruple bonds.[6] Magnetic studies of the μ-thiolato dimers led to the first direct magnetic detection of a $^3(\delta\delta^*)$ excited triplet state. This finding prompted us to undertake further studies of the structures and temperature-dependent magnetic properties of related Mo_2^{6+} and W_2^{6+} compounds. The preparation of these d^3–d^3 dimers has been achieved via reactions of the types summarized in Scheme I.

In the present study we have prepared the μ-chloro complexes $M_2Cl_6(dppe)_2$ (M = Mo, W; dppe = $Ph_2PCH_2CH_2PPh_2$) from the oxidative addition of chlorine to the quadruple bonds of α- or β-$M_2Cl_4(dppe)_2$. A related molecule containing the asymmetric bidentate phosphine $Et_2PCH_2CH_2PPh_2$ (dedppe) was isolated from a dichloromethane solution of α-$Mo_2Cl_4(dedppe)_2$. Evidently, oxidation is promoted by the halogenated solvent in this case.

The title compounds constitute the newest members of the homologous series $M_2Cl_6(dppe)_2$ where M = Zr,[7] Nb,[8] Mo, W, or Re.[9] These complexes are intriguing because, despite their simplicity, the factors that influence the M–M bonding in these molecules are not well understood. A theoretical treatment of this structural type was published by Shaik and Hoffmann in 1980,[10] and although the work accounted for the absence of a Re–Re interaction in $Re_2Cl_6(dppe)_2$, it cannot explain our recent findings that metal–metal-bonded complexes with the *same* formula exist for transition elements from groups 4–6. In an effort to learn more about this interesting system, we have carried out single-crystal studies and variable-temperature magnetic susceptibility measurements on $M_2Cl_6(dppe)_2$ (M = Mo, W). The electrochemistry and the infrared and electronic spectra of the

Scheme I

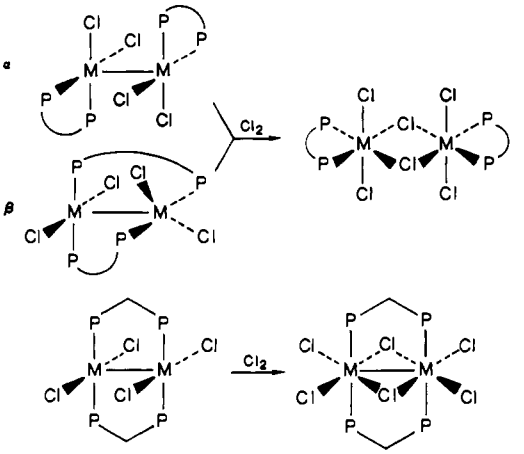

(1) (a) Texas A&M University. (b) University of New Orleans.
(2) (a) Cotton, F. A.; Duraj, S. A.; Roth, W. J. *J. Am. Chem. Soc.* **1984**, *106*, 4749. (b) Campbell, G. C.; Canich, J. M.; Cotton, F. A.; Duraj, S. A.; Haw, J. F. *Inorg. Chem.* **1986**, *25*, 287.
(3) Chisholm, M. H.; Kirkpatrick, C. C.; Huffman, J. C. *Inorg. Chem.* **1981**, *20*, 871.
(4) Cotton, F. A.; Shamshoum, E. S. *J. Am. Chem. Soc.* **1984**, *106*, 3222.
(5) Cotton, F. A.; Dunbar, K. R. *Inorg. Chem.* **1987**, *26*, 1305.
(6) (a) Cotton, F. A.; Powell, G. L. *J. Am. Chem. Soc.* **1984**, *106*, 3371. (b) Cotton, F. A.; Diebold, M. P.; O'Connor, C. J.; Powell, G. L. *J. Am. Chem. Soc.* **1985**, *107*, 7438.
(7) Cotton, F. A.; Diebold, M. P.; Kibala, P.; Roth, W. J., unpublished work.
(8) Cotton, F. A.; Roth, W. J. *Inorg. Chim. Acta* **1983**, *71*, 175.
(9) Cotton, F. A.; Curtis, N. F.; Robinson, W. R. *Inorg. Chem.* **1965**, *4*, 1696.
(10) Shaik, S.; Hoffmann, R. *J. Am. Chem. Soc.* **1980**, *102*, 1194.

0020-1669/87/1326-4051$01.50/0

dimolybdenum analogue were also investigated.

Experimental Section

Starting Materials. α- and β-$Mo_2Cl_4(dppe)_2$ were prepared from the reaction of $Mo_2(\mu\text{-}O_2CCH_3)_4$, Me_3SiCl, and dppe in refluxing THF according to a previously reported method.[11-13] A mixture of α- and β-$W_2Cl_4(dppe)_2$ was prepared by a literature procedure.[14,15] WCl_6, used to prepare the WCl_4, was purchased from Aldrich Chemicals. 1,2-Bis(diphenylphosphino)ethane (dppe) and 1-(diethylphosphino)-2-(diphenylphosphino)ethane (dedppe) were purchased from Strem Chemicals and used as received. Chlorine gas was supplied by Matheson Gas Products.

Reaction Procedures. Unless otherwise stated, all operations were carried out under an atmosphere of dry argon. Solvents were dried by conventional methods and distilled under dinitrogen.

Preparation of $Mo_2Cl_6(dppe)_2$. Method 1. 0.400 g (0.354 mmol) of β-$Mo_2Cl_4(dppe)_2$ was suspended in 30 mL of CH_2Cl_2 in a beaker, and a small amount of chlorine gas was introduced into the solution. The pale salmon suspension immediately dissolved to give a red solution, which was filtered and allowed to evaporate slowly to a low volume in air. Orange-red crystals grew in bunches on the bottom and sides of the beaker; these were filtered off, washed with diethyl ether, and dried under reduced pressure. Yield: 0.39 g (91%). Anal. Calcd for $C_{52}H_{48}Cl_6P_4Mo_2$: C, 51.98; H, 4.03. Found: C, 51.54; H, 3.76. IR spectrum, CsI plates (Nujol mull): 1575 w, 1560 w, 1475 m, 1425 s, 1405 m, 1325 w, 1300 w, 1265 w, 1180 m, 1150 w, 1090 s, 1020 m, 990 m, 900 w, 860 m, 820 m, 735 s, 680 s, 670 m, 645 m, 515 s, 490 m, 470 m, 430 br, 330 s cm^{-1} (br = broad, s = strong, m = medium, w = weak).

Method 2. A 50-mL three-neck flask was charged with 0.200 g (0.177 mmol) of green α-$Mo_2Cl_4(dppe)_2$ and 15 mL of CH_2Cl_2. Chlorine gas, at a medium flow rate, was bubbled into the mixture for ~15 s, and the initial green suspension quickly reacted to yield a purple solution. After being stirred for 1 h at room temperature, the reaction solution was a pale red color and crystals had formed on the walls of the flask. The material was filtered off in air, and the filtrate was reduced in volume to yield another crop of microcrystals. The combined product was washed with diethyl ether and dried. Yield: 0.19 g (89%). The spectroscopic and electrochemical properties of this material were identical with those found for the complex formed by using method 1.

Preparation of $Mo_2Cl_6(dedppe)_2$ (2). This compound was obtained upon prolonged storage of $Mo_2Cl_4(dedppe)_2$ in CH_2Cl_2 solution. The chemistry of this process, which is reproducible, is a subject of continuing investigation.

Preparation of $W_2Cl_6(dppe)_2$. Method 1. A suspension of WCl_4 (1.5 g, 4.6 mmol) was stirred together with 2.5 mL of a Na/Hg amalgam (2 mmol/mL) in 25 mL of THF at −20 °C. After 30 min, the reaction was allowed to warm to room temperature. The yellow-green THF solution of $W_2Cl_6(THF)_4$ was filtered through Celite under argon, and the residue was extracted with fresh THF to dissolve the precipitate. The volume of the combined filtrate and washings was reduced to ~30 mL, 1.8 g (~4.6 mmol) of dppe was added, and the solution was heated to reflux for 15 min and then stirred at room temperature for 1 h. The red solution was reduced in volume, and hexane was added to initiate precipitation. A rose solid was filtered off and washed with ethanol followed by diethyl ether. Yield: 2.7 g (87%). Anal. Calcd for $C_{52}H_{48}Cl_6P_4W_2$: C, 45.35; H, 3.51. Found: C, 45.66; H, 3.79.

Method 2. A sample of $W_2Cl_4(dppe)_2$ (0.100 g, 0.076 mmol) that contained both α and β isomers was treated with a small amount of chlorine gas in ~5 mL of CH_2Cl_2. The initial brown color turned red very quickly, with the precipitation of a pale red solid, which was filtered off under argon and washed with diethyl ether. Yield: 0.071 g (68%). An IR spectrum of the product was identical with that reported for the compound isolated by method 1.

Preparation of Single Crystals. Suitable crystals of $Mo_2Cl_6(dppe)_2 \cdot 4CH_2Cl_2$ (**1**) and $W_2Cl_6(dppe)_2 \cdot 4CH_2Cl_2$, (**3**) were obtained by slow evaporation of dichloromethane solutions of the compounds. A single crystal of **2** was isolated from a dichloromethane solution of α-$Mo_2Cl_4(dedppe)_2$.

X-ray Structure Analysis. Data Collection and Reduction. A thin crystal of **1** (with approximate dimensions 0.55 × 0.50 × 0.20 mm) was glued inside of a glass capillary and surrounded by mother liquor. Crystals of **2** (0.20 × 0.20 × 0.30 mm) and **3** (0.20 × 0.20 × 0.15 mm) were mounted at the ends of glass fibers. Geometric and intensity data were collected on an Enraf-Nonius CAD-4F autodiffractometer for **1** and **3** and on a Nicolet P3 four-circle diffractometer in the case of **2**. The experiment was done at room temperature for **1** and **2** and at −106 °C for **3**. The procedures employed for data collection have been described previously.[16] For each of the three structures the unit cell parameters and orientation matrix were refined by a least-squares fit to the positions of 25 reflections. The lattice dimensions and Laue symmetry were verified by photography.

For compound **1** the ω-scan technique was used to scan data points in the range $4 \le 2\theta \le 47°$. An ω–2θ scan was used to collect data for **2** and **3** in the range $4 \le 2\theta \le 45°$. In all three structures, three check reflections monitored throughout data collection displayed no significant gain or loss in intensity. Data reduction was carried out by using well-established computational procedures.[17] The data were corrected for Lorentz and polarization effects, and azimuthal scans (ψ scans) of reflections having an Eulerian angle χ near 90° were used as a basis for empirical absorption corrections.[18] Pertinent crystallographic parameters for **1–3** are summarized in Table I.

Structure Solution and Refinement. $Mo_2Cl_6(dppe)_2 \cdot 4CH_2Cl_2$ (1). The molecular unit of chemical interest, $Mo_2Cl_6(dppe)_2$, was developed and refined without complication, in an alternating series of least-squares cycles and difference Fourier maps. In addition to the molecule of interest, there were three regions of the unit cell containing CH_2Cl_2 molecules. We have called these sections A, B, and C, and the atoms are named accordingly (Table II). The C molecule is on a crystallographic mirror plane and is not disordered. The molecule in the A region was modelled in the final refinement with an occupancy of $^1/_6$—a value we arrived at after refining multiplicities in earlier cycles. The B region is disordered to the extent that, from the atomic sites that we located and refined, we can assemble as many as nine different, partially occupied CH_2Cl_2 molecules with acceptable geometry. We cannot deconvolute this pattern unambiguously, nor do we have any wish to do so. We arrived at site occupancies for the final refinement by refining them in earlier cycles. The total occupancy factor for the three discrete carbon sites in the B region is $^1/_3$, and the total occupancy for the three discrete chlorine sites is $^2/_3$.

In the refinement of parameters for the three solvent regions, loose geometrical restraints were used for all of the C–Cl bonds in the CH_2Cl_2 moieties. This led to as smooth a refinement as can be expected in such a case. The refinement of parameters for the solvent region oscillated, with some parameters changing by 3σ in alternate directions in successive cycles. No parameter in the molecular complex under study was changed by more than 0.37σ in the final least-squares cycle.

The total population of CH_2Cl_2 molecules in the unit cell was modeled as 8—with site occupancies of $^1/_6$, $^1/_3$, and $^1/_2$ for the A, B, and C regions, respectively. We have calculated the relevant quantities in Table I accordingly, with a stoichiometry of $Mo_2Cl_6(dppe)_2 \cdot 4CH_2Cl_2$ and $Z = 2$. We do not claim that no variation of our model exists that can fit the diffraction data equally well. Indeed, it is by no means clear that the composition of the crystal, particularly in the B region, remained constant during the course of data collection. We did observe, during the course of refining several models for the disordered CH_2Cl_2 molecules, that variations in this part of the overall model did not affect the refinement of the $Mo_2Cl_6(dppe)_2$ molecule.

The refinement finished with least-squares residuals of $R = 0.0694$, $R_w = 0.0718$, and quality-of-fit = 2.21. These and other quantities are defined and summarized in Table I.

$Mo_2Cl_6(dedppe)_2 \cdot 2CH_2Cl_2$ (2). The space group was determined to be $P2_1/c$ based upon systematic absences. The structure was solved by using the direct-methods program MULTAN, which gave the position of the unique molybdenum atom. The rest of the atoms were located by using a series of difference Fourier maps alternating with least-squares refinement of the atoms found. In the end, 241 parameters were refined to 1311 unique data with $F_o^2 \ge 3\sigma(F_o^2)$. Anisotropic thermal parameters were used for all atoms except those of the two dichloromethane solvent molecules. The final weighted R factor was 0.079 and the unweighted R factor was 0.064. These and other figures of merit are listed in Table I.

$W_2Cl_6(dppe)_2 \cdot 4CH_2Cl_2$ (3). The triclinic cell of **3** consists of two independent dimers, the midpoints of which reside on crystallographic

(11) Agaskar, P. A.; Cotton, F. A. *Inorg. Chem.* **1984**, *23*, 3383.
(12) Campbell, F. L., III; Cotton, F. A.; Powell, G. L. *Inorg. Chem.* **1984**, *23*, 4222.
(13) Campbell, F. L., III; Cotton, F. A.; Powell, G. L. *Inorg. Chem.* **1985**, *24*, 177.
(14) Sharp, P. R.; Schrock, R. R. *J. Am. Chem. Soc.* **1980**, *102*, 1430.
(15) Schrock, R. R.; Sturgeoff, L. G.; Sharp, P. R. *Inorg. Chem.* **1983**, *22*, 2801.
(16) Cotton, F. A.; Frenz, B. A.; Deganello, G.; Shaver, A. *J. Organomet. Chem.* **1973**, *50*, 227.
(17) Data processing was done on a PDP-11/60 computer with PDP-11-simulated VAXSDP and on a VAX-11/780 computer with programs from the package VAXSDP.
(18) North, A. C. T.; Phillips, D. C.; Mathews, F. S. *Acta Crystallogr., Sect. A: Cryst. Phys., Diffr., Theor. Gen. Crystallogr.* **1968**, *A24*, 351.

Table I. Crystal Data for **1–3**

	1	2	3
formula	$Mo_2Cl_{14}P_4C_{56}H_{56}$	$Mo_2Cl_{10}P_4C_{38}H_{52}$	$W_2Cl_{14}P_4C_{56}H_{56}$
fw	1541.2	1179.14	1717.01
space group	$C2/m$	$P2_1/c$	$P\bar{1}$
syst absences	(hkl), $h + k \neq 2n$	$0k0$, $k \neq 2n + 1$; $h0l$, $l \neq 2n + 1$	
a, Å	17.288 (2)	12.148 (6)	12.521 (2)
b, Å	18.500 (2)	10.707 (5)	13.956 (3)
c, Å	13.855 (4)	22.529 (5)	20.690 (5)
α, deg	90.0	90.0	104.36 (4)
β, deg	121.14 (2)	101.57 (4)	92.34 (3)
γ, deg	90.0	90.0	112.34 (4)
V, Å^3	3793 (3)	2870 (4)	3202 (4)
Z	2	2	2
d_{calcd}, g/cm^3	1.35	1.36	1.78
cryst size, mm	0.55 × 0.50 × 0.20	0.20 × 0.20 × 0.30	0.20 × 0.20 × 0.15
μ(Mo Kα), cm^{-1}	9.29	10.30	43.92
data collcn instrument	Enraf-Nonius CAD-4F	Syntex P3	Enraf-Nonius CAD-4F
radiation (monochromated in incident beam)	Mo Kα (λ_α = 0.71073 Å)	Mo Kα (λ_α = 0.71073 Å)	Mo Kα (λ_α = 0.71073 Å)
orientation reflcns: no.; range (2θ), deg	25; 20–30	25; 10–20	25; 20–30
temp, °C	22 ± 2	22 ± 3	−106
scan method	ω scans	ω–2θ	ω–2θ
data collcn range (2θ), deg	4–47	4–45	4–45
no. of unique data, total	3853	1603	7886
no. of data with $F_o^2 > 3\sigma(F_o^2)$	2712	1311	5468
no. of params refined	181	241	665
obsd transmissn factors: max, min	1.00, 0.89	0.99, 0.88	0.99, 0.86
R^a	0.0694	0.064	0.0441
$R_w{}^b$	0.0718	0.079	0.0538
quality-of-fit indicator^c	2.21	1.56	1.36
largest shift/esd, final cycle	0.37 (See text)	0.87	0.50
largest peak, e/Å^3	1.2	1.1	1.2

$^a R = \sum||F_o| - |F_c||/\sum|F_o|$. $^b R_w = [\sum w(|F_o| - |F_c|)^2/\sum w|F_o|^2]^{1/2}$; $w = 1/\sigma^2(|F_o|)$. ^{c}Quality-of-fit = $[\sum w(|F_o| - |F_c|)^2/(N_{observns} - N_{paras})]^{1/2}$.

Table II. Atomic Positional Parameters and Equivalent Isotropic Displacement Parameters (Å^2) and Their Estimated Standard Deviations for $Mo_2Cl_6(dppe)_2 \cdot 4CH_2Cl_2$ (**1**)^a

atom	x	y	z	B
Mo(1)	0.000	0.07464 (5)	0.000	2.28 (2)
Cl(1)	0.0988 (2)	0.000	0.1605 (2)	3.06 (6)
Cl(2)	0.1120 (1)	0.0915 (1)	−0.0502 (2)	3.69 (5)
P(1)	0.0802 (1)	0.1795 (1)	0.1360 (2)	3.26 (5)
C(1)	0.0145 (7)	0.2611 (5)	0.0622 (7)	5.4 (3)
C(2)	0.1972 (5)	0.1967 (5)	0.1782 (6)	4.4 (2)
C(3)	0.2619 (6)	0.1503 (6)	0.2534 (9)	5.5 (3)
C(4)	0.3558 (7)	0.1592 (8)	0.295 (1)	7.4 (3)
C(5)	0.3784 (7)	0.214 (1)	0.249 (1)	10.2 (4)
C(6)	0.3171 (8)	0.2614 (9)	0.173 (1)	11.3 (4)
C(7)	0.2193 (7)	0.2556 (7)	0.133 (1)	8.1 (3)
C(8)	0.0884 (5)	0.1851 (5)	0.2740 (6)	3.8 (2)
C(9)	0.0598 (6)	0.1304 (6)	0.3128 (7)	5.0 (2)
C(10)	0.0707 (7)	0.1389 (8)	0.4208 (8)	6.9 (3)
C(11)	0.1078 (7)	0.1988 (8)	0.4844 (8)	6.6 (3)
C(12)	0.1357 (6)	0.2541 (8)	0.4454 (8)	6.7 (3)
C(13)	0.1259 (6)	0.2478 (6)	0.3371 (8)	5.4 (3)
C(1A)	0.370 (3)	−0.07 (1)	0.573 (8)	16*
Cl(1A)	0.269 (2)	0.000	0.494 (3)	16*
Cl(2A)	0.440 (2)	0.000	0.538 (3)	16*
C(1B)	0.288 (1)	0.500	0.223 (1)	15.4 (4)*
C(2B)	0.351 (2)	0.412 (1)	0.36 (3)	15.5 (4)*
C(3B)	0.341 (5)	0.420 (6)	0.25 (3)	15.4 (4)*
Cl(1B)	0.390 (1)	0.500	0.327 (2)	15.5 (4)*
Cl(2B)	0.390 (1)	0.500	0.346 (1)	15.5 (4)*
Cl(3B)	0.233 (1)	0.426 (1)	0.230 (2)	15.5 (4)*
C(1C)	0.158 (2)	0.500	−0.107 (3)	12*
Cl(1C)	0.1182 (8)	0.4286 (7)	−0.069 (1)	25.6 (5)*

^{a}Asterisks denote displacement parameters for atoms refined isotropically. The A and B solvent regions (see text) were refined with group displacement parameters. The displacement parameters for anisotropically refined atoms are given in the form of the equivalent isotropic displacement parameter defined as $^4/_3[a^2\beta_{11} + b^2\beta_{22} + c^2\beta_{33} + ab(\cos\gamma)\beta_{12} + ac(\cos\beta)\beta_{13} + bc(\cos\alpha)\beta_{23}]$.

inversion centers. The locations of the two unique W atoms were determined from a Patterson map, and successive iterations of least-squares refinement and difference Fourier maps led to the identification of all atomic positions. All atoms except C(14), C(25), C(28), and C(31) were refined with anisotropic thermal parameters.

In all, 665 parameters were fitted to 5468 observations. The final least-squares cycle did not shift any parameter by more than 0.50 times its estimated standard deviation. The final residuals are $R = 0.0441$ and $R_w = 0.0538$.

Magnetic Measurements. Polycrystalline samples of the complexes were measured with a superconducting SQUID susceptometer operating at a measuring field of 2.0 kOe. Measurement and calibration techniques are reported elsewhere.[19] The sample holders were fabricated from Delrin, and the magnetism of the sample holder was checked over the entire temperature range (6–400 K). The magnetic data were corrected at each temperature for the corresponding magnetic contribution of the sample bucket. A listing of the molar magnetic susceptibility data for each of the complexes corrected for the contribution of the sample bucket and for the diamagnetism of the constituent atoms using Pascal's constants is given in the supplementary material.

Physical Measurements. Electronic spectra were measured on dichloromethane solutions with a Cary 17D spectrophotometer. Electrochemical measurements were performed with a Bioanalytical Systems, Inc., Model BAS 100 electrochemical analyzer in conjunction with a Bausch & Lomb, Houston Instruments Model DMP 40 digital plotter. Experiments were carried out in dichloromethane solutions that contain 0.2 M tetra-*n*-butylammonium hexafluorophosphate (TBAH) as a supporting electrolyte. A three-electrode cell configuration was used, with a platinum disk, Model BAS MF 2032, and a platinum wire as working and auxiliary electrodes, respectively. A BAS MF 2020 Ag/AgCl cell was used a reference electrode (against which ferrocene is oxidized at +0.52 V). All potentials were referenced to the Ag/AgCl electrode at 22 ± 2 °C with a full positive feedback resistance compensation and are uncorrected for junction potentials. $E_{1/2}$ values were determined as $(E_{p,a} + E_{p,c})/2$. Infrared spectra were recorded as Nujol mulls between CsI plates with the use of a Perkin-Elmer 785 spectrophotometer. Elemental analyses were performed by Galbraith Laboratories, Inc.

Results and Discussion

Synthetic Details. The reactions of quadruply bonded α,β-$Mo_2Cl_4(dppe)_2$ with Cl_2 proceed rapidly at room temperature to yield the oxidative-addition product $Mo_2(\mu\text{-}Cl)_2Cl_4(dppe)_2$. Yields are high (>85%) provided the reactions are done in CH_2Cl_2 without a large excess of Cl_2. Upon prolonged exposure to

(19) O'Connor, C. J. *Prog. Inorg. Chem.* **1982**, *29*, 203 and references cited therein.

Table III. Atomic Positional Parameters and Equivalent Isotropic Displacement Parameters (Å²) and Their Estimated Standard Deviations for $Mo_2Cl_6(dedppe)_2 \cdot 2CH_2Cl_2$ (**2**)

atom	x	y	z	B[a]
Mo(1)	0.9272 (1)	0.0994 (2)	1.00259 (8)	2.76 (3)
Cl(1)	1.0031 (4)	0.0442 (5)	0.9153 (2)	3.5 (1)
Cl(2)	0.7582 (4)	−0.0180 (6)	0.9697 (2)	4.0 (1)
Cl(3)	1.0653 (4)	0.2603 (5)	1.0340 (2)	4.2 (1)
Cl(4)	0.3938 (8)	0.338 (1)	−0.0038 (5)	12.1 (3)*
Cl(5)	0.275 (1)	0.343 (1)	−0.1251 (5)	14.3 (4)*
Cl(6)	0.432 (1)	0.363 (1)	0.1647 (6)	16.3 (4)*
Cl(7)	0.3487 (9)	0.145 (1)	0.2144 (5)	13.4 (3)*
P(1)	0.8202 (4)	0.2006 (6)	1.0766 (2)	3.6 (1)
P(2)	0.8184 (5)	0.2640 (6)	0.9340 (3)	4.5 (2)
C(1)	0.739 (2)	0.336 (2)	1.0369 (8)	4.6 (6)
C(2)	0.698 (2)	0.306 (3)	0.968 (1)	7.2 (8)
C(3)	0.722 (2)	0.103 (2)	1.1070 (8)	4.2 (5)
C(4)	0.611 (2)	0.088 (3)	1.075 (1)	6.0 (6)
C(5)	0.536 (2)	0.008 (2)	1.099 (1)	6.5 (7)
C(6)	0.570 (2)	−0.050 (3)	1.154 (1)	6.9 (8)
C(7)	0.676 (2)	−0.030 (3)	1.186 (1)	7.0 (7)
C(8)	0.754 (2)	0.043 (2)	1.163 (1)	5.0 (6)
C(9)	0.897 (2)	0.274 (2)	1.1479 (8)	4.0 (5)
C(10)	1.004 (2)	0.233 (2)	1.1709 (8)	4.0 (6)
C(11)	1.059 (2)	0.279 (3)	1.230 (1)	6.6 (7)
C(12)	0.999 (2)	0.367 (3)	1.258 (1)	7.0 (7)
C(13)	0.891 (2)	0.407 (2)	1.2316 (9)	5.9 (6)
C(14)	0.835 (2)	0.356 (2)	1.1768 (9)	4.9 (6)
C(15)	0.885 (2)	0.413 (3)	0.920 (1)	7.1 (7)
C(16)	0.966 (2)	0.399 (3)	0.881 (1)	9.3 (8)
C(17)	0.746 (2)	0.206 (2)	0.856 (1)	6.8 (7)
C(18)	0.670 (2)	0.293 (3)	0.819 (1)	8.7 (9)
C(19)	0.295 (2)	0.260 (3)	−0.056 (1)	6.9 (7)*
C(20)	0.334 (3)	0.236 (4)	0.152 (2)	12 (1)*

[a] Starred values denote isotropically refined atoms. Values for anisotropically refined atoms are given in the form of the equivalent isotropic displacement parameter defined as $^4/_3[a^2\beta_{11} + b^2\beta_{22} + c^2\beta_{33} + ab(\cos\gamma)\beta_{12} + ac(\cos\beta)\beta_{13} + bc(\cos\alpha)\beta_{23}]$.

chlorinated solutions, the red Mo_2^{6+} species decomposes to a colorless material, most likely a high oxidation state monomer.

The isolation of $W_2Cl_6(dppe)_2$ was achieved by two separate routes. Oxidative addition is not practical for bulk synthesis because the starting material α,β-$W_2Cl_4(dppe)_2$ is prepared in fairly low yield from a substitution reaction involving $W_2Cl_4(P\text{-}n\text{-}Bu_3)_4$,[14] a compound that is also difficult to isolate and purify. A more direct synthetic strategy is the addition of dppe to a solution of $W_2Cl_6(THF)_4$. The latter species is easily generated by treating WCl_4 with 1 equiv of a sodium amalgam in THF. Walton and co-workers have recently reported the synthesis of $W_2Cl_6(dppm)_2$ by this route.[20]

Compounds **1** and **3** are moderately soluble in a variety of common solvents including dichloromethane, acetone, and benzene. The complexes are quite air stable both in the solid state and in solution. These properties are in marked contrast to those exhibited by the analogous dirhenium species $Re_2Cl_6(dppe)_2$.[9]

The formation of compound **2** occurred spontaneously when $Mo_2Cl_4(dedppe)_2$, as a mixture of α and β isomers, was subjected to slow recrystallization from CH_2Cl_2 solution. As will be explained in detail in a later publication dealing with other cases, we believe that CH_2Cl_2 often serves as a chlorinating agent (effectively as a supplier of two Cl atoms), although the other products of this sort of process are unknown, and its mechanism is not understood.

Molecular Structures. The three new $M_2Cl_6(P\text{-}P)_2$ compounds reported in this paper have been characterized by X-ray crystallography. The molecules possess geometries based on an edge-sharing bioctahedral arrangement of the core atoms. In all cases the central $M_2Cl_6P_4$ unit has essentially the same structure, in which the equatorial plane is occupied by chelating phosphine groups and μ-Cl ligands and the four apical positions are filled by terminal chloride ligands. The virtual symmetry of this central $M_2Cl_6P_4$ set is thus D_{2h}. The bond angles around the metal atoms are those of an octahedral arrangement distorted in the usual manner because of the presence of M–M bonding, viz., opening of the (μ-Cl)–M–(μ-Cl) angle and deviation from linearity of the angle Cl_t–M–Cl_t.[21]

The atomic positional parameters for the three compounds are listed in Tables II–IV. Tables V–VII give selected bond distances

Table IV. Selected Atomic Positional Parameters and Equivalent Isotropic Displacement Parameters (Å²) and Their Estimated Standard Deviations for $W_2Cl_6(dppe)_2 \cdot 4CH_2Cl_2$ (**3**)[a,b]

atom	x	y	z	B
W(1)	0.10285 (4)	0.05098 (4)	0.04098 (2)	1.13 (1)
W(2)	0.10962 (4)	0.57248 (4)	0.50529 (3)	1.29 (1)
Cl(1)	0.0577 (3)	0.1856 (2)	0.1165 (2)	1.86 (7)
Cl(2)	0.2002 (3)	−0.0556 (2)	−0.0168 (2)	1.76 (7)
Cl(3)	0.0608 (3)	0.0942 (2)	−0.0600 (2)	1.61 (7)
Cl(4)	0.2021 (3)	0.4490 (2)	0.4729 (2)	1.98 (7)
Cl(5)	0.0745 (3)	0.7331 (2)	0.5382 (2)	1.84 (7)
Cl(6)	0.0325 (3)	0.4972 (2)	0.5944 (2)	1.76 (7)
P(1)	0.2982 (3)	0.2062 (3)	0.0531 (2)	1.85 (8)
P(2)	0.1990 (3)	0.0386 (3)	0.1470 (2)	1.68 (8)
P(3)	0.2449 (3)	0.6690 (3)	0.4332 (2)	1.72 (8)
P(4)	0.2885 (3)	0.6783 (3)	0.5944 (2)	1.81 (8)

[a] See footnote *a* in Table II. [b] Parameters for phenyl carbon atoms are listed in the supplementary material.

Table V. Selected Bond Distances (Å) and Angles (deg) and Their Estimated Standard Deviations[a] for $Mo_2Cl_6(dppe)_2 \cdot 4CH_2Cl_2$

	Distances		
Mo(1)–Mo(1)′	2.762 (1)	P(1)–C(1)	1.847 (9)
Mo(1)–Cl(1)	2.417 (2)	P(1)–C(2)	1.820 (9)
Mo(1)–Cl(2)	2.392 (2)	P(1)–C(8)	1.846 (10)
Mo(1)–P(1)	2.556 (2)	C(1)–C(1)′	1.525 (15)
	Angles		
Mo(1)′–Mo(1)–Cl(1)	55.16 (3)	Mo(1)–P(1)–C(1)	105.6 (3)
Mo(1)′–Mo(1)–Cl(2)	97.51 (5)	Mo(1)–P(1)–C(2)	117.3 (3)
Mo(1)′–Mo(1)–P(1)	139.38 (4)	Mo(1)–P(1)–C(8)	121.9 (3)
Cl(1)–Mo(1)–Cl(1)′	110.32 (5)	C(1)–P(1)–C(2)	107.3 (5)
Cl(1)–Mo(1)–Cl(2)	92.81 (9)	C(1)–P(1)–C(8)	102.9 (5)
Cl(1)–Mo(1)–Cl(2)′	95.76 (9)	C(2)–P(1)–C(8)	100.3 (4)
Cl(1)–Mo(1)–P(1)	84.23 (5)	P(1)–C(1)–C(1)′	112.0 (7)
Cl(1)–Mo(1)–P(1)′	165.39 (6)	P(1)–C(2)–C(3)	118.1 (8)
Cl(2)–Mo(1)–Cl(2)′	164.97 (8)	P(1)–C(2)–C(7)	120.4 (6)
Cl(2)–Mo(1)–P(1)	84.44 (8)	C(3)–C(2)–C(7)	121.5 (9)
Cl(2)–Mo(1)–P(1)′	84.16 (8)	P(1)–C(8)–C(9)	121.4 (7)
P(1)–Mo(1)–P(1)′	81.25 (6)	P(1)–C(8)–C(13)	117.2 (8)
Mo(1)–Cl(1)–Mo(1)′	69.68 (6)	C(9)–C(8)–C(13)	121.3 (9)

[a] Numbers in parentheses are estimated standard deviations in the least significant digits.

Table VI. Selected Bond Distances (Å) and Angles (deg) and Their Estimated Standard Deviations for $Mo_2Cl_6(dedppe)_2 \cdot 2CH_2Cl_2$ (**2**)

	Distances		
Mo(1)′–Mo(1)	2.785 (3)	Mo(1)–Cl(3)	2.410 (6)
Mo(1)–Cl(1)	2.424 (5)	Mo(1)–P(1)	2.552 (6)
Mo(1)–Cl(2)	2.396 (5)	Mo(1)–P(2)	2.535 (6)
	Angles		
Mo(1)′–Mo(1)–Cl(1)	55.1 (1)	P(1)–Mo(1)–P(2)	80.3 (2)
Mo(1)′–Mo(1)–Cl(1)′	54.5 (1)	Cl(1)–Mo(1)–Cl(1)′	109.6 (2)
Mo(1)′–Mo(1)–Cl(2)	95.6 (2)	Cl(1)–Mo(1)–Cl(2)	93.6 (2)
Mo(1)′–Mo(1)–Cl(3)	98.5 (2)	Cl(1)–Mo(1)–Cl(3)	93.3 (2)
Mo(1)′–Mo(1)–P(1)	139.7 (2)	Cl(1)–Mo(1)–P(1)	165.2 (2)
Mo(1)′–Mo(1)–P(2)	139.8 (2)	Cl(1)–Mo(1)–P(2)	84.9 (2)
Cl(2)–Mo(1)–Cl(3)	165.8 (2)	Cl(1)′–Mo(1)–Cl(2)	92.8 (2)
Cl(2)–Mo(1)–P(1)	84.7 (2)	Cl(1)′–Mo(1)–Cl(3)	96.5 (2)
Cl(2)–Mo(1)–P(2)	82.3 (2)	Cl(1)′–Mo(1)–P(1)	85.2 (2)
Cl(3)–Mo(1)–P(1)	85.4 (2)	Cl(1)′–Mo(1)–P(2)	165.1 (2)
Cl(3)–Mo(1)–P(2)	86.0 (2)		

(20) Fanwick, P. E.; Harwood, W. S.; Walton, R. A. *Inorg. Chem.* **1987**, *26*, 242.

(21) (a) Cotton, F. A.; Ucko, D. *Inorg. Chim. Acta* **1972**, *6*, 161. (b) Cotton, F. A.; *Polyhedron* **1987**, *6*, 667.

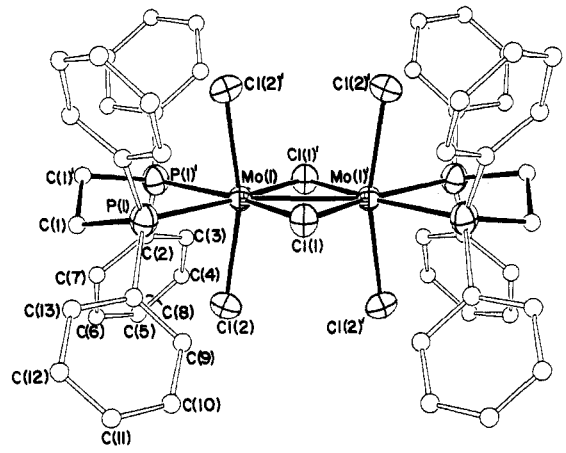

Figure 1. ORTEP view of the structure of $Mo_2Cl_6(dppe)_2$ (**1**) with thermal ellipsoids drawn at the 50% probability level. Phenyl group carbon atoms are shown as small circles for clarity.

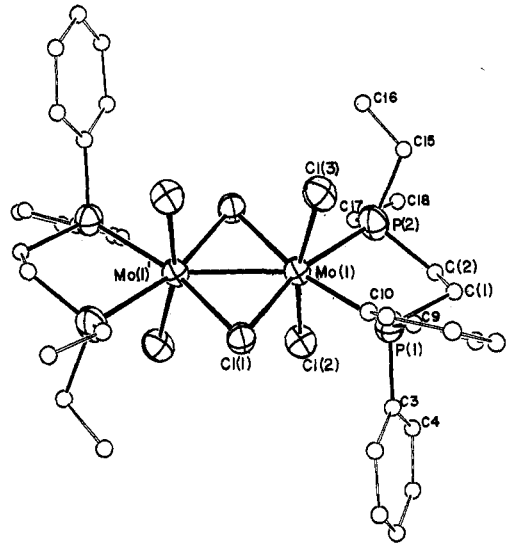

Figure 2. ORTEP diagram of the entire molecule of $Mo_2Cl_6(dedppe)_2$. Thermal ellipsoids of the Mo, Cl, and P atoms are represented at the 50% probability level, and those of the carbon atoms have been arbitrarily reduced.

and angles for **1–3**, respectively.

Compound **1**, $Mo_2Cl_6(dppe)_2 \cdot 4CH_2Cl_2$, crystallizes in the monoclinic space group $C2/m$ with $Z = 2$. The crystallographic symmetry is $2/m$ (C_{2h}); the molecular symmetry closely approximates D_{2h}. The ORTEP diagram in Figure 1 illustrates this point. The edge-sharing bioctahedron is bridged by two chlorine atoms that form an acute angle Mo(1)–Cl(1)–Mo(1)′ = 69.68 (6)° and an obtuse angle Cl(1)–Mo(1)–Cl(1)′ = 110.32 (5)°, which taken along with the Mo(1)–Mo(1)′ distance of 2.762 (1) Å clearly indicate the presence of M–M bonding. A repulsive effect between neighboring apical chlorine atoms is evidenced by the Cl(2)–Mo(1)–Cl(2)′ angle of 164.97 (8)°, which deviates approximately 15° from the 180° angle expected in the absence of such an effect. We have noticed this distortion in the structures of other compounds of the type $(L\text{–}L)Cl_2M(\mu\text{-}X)_2MCl_2(L\text{–}L)$ including the μ-thiolato compounds.[7]

Interestingly, we do not observe a decrease in the Cl_t–Mo–Cl_t angle (i.e., a greater deviation from linearity) with decreasing Mo–Mo distance, as one might predict based upon steric arguments alone. In fact, the opposite trend is seen when comparing $Mo_2Cl_6(dppe)_2$ and $Mo_2Cl_4(\mu\text{-}SEt)_2(dmpe)_2$ for which the Mo–Mo distances are 2.762 (1) and 2.712 (3) Å, but the Cl_t–Mo–Cl_t angles are 164.97 (6) and 162.9 (2)°, respectively. No doubt in both cases the Cl···Cl repulsions are close to the maximum tolerable value and thus other, secondary factors can exert influences that are small and difficult to predict.

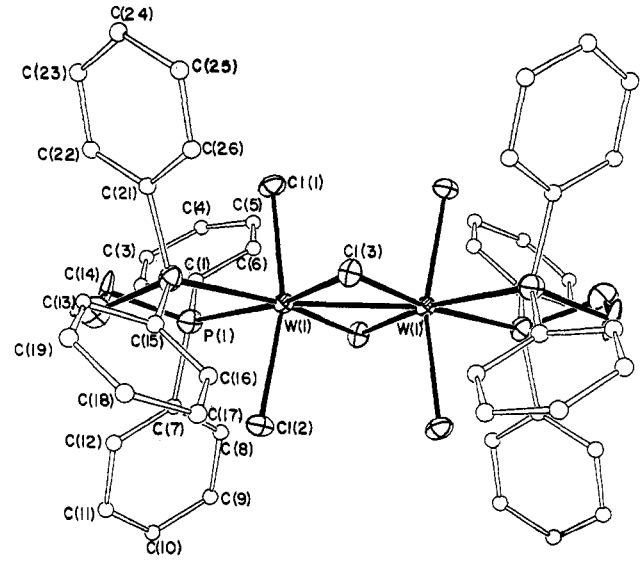

Figure 3. Structure and labeling scheme of one of the independent molecules in the crystal structure of $W_2Cl_6(dppe)_2$. Atoms are represented by their 50% probability ellipsoids. The phenyl ring carbon atoms are depicted as small circles.

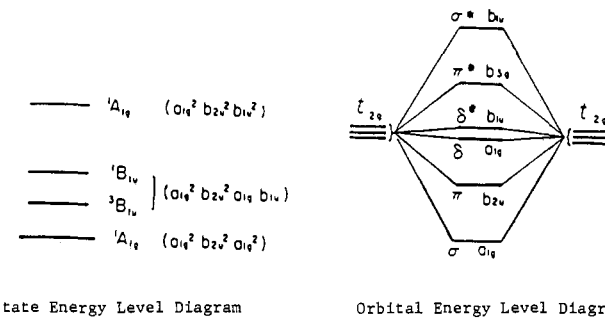

Figure 4. Qualitative orbital and state energy level diagrams for the case where $E(\delta) < E(\delta^*)$.

Other distances (Mo(1)–P(1) = 2.556 (2), Mo(1)–Cl(1) = 2.417 (2), Mo(1)–Cl(2) = 2.392 (2) Å) and angles (P(1)–Mo(1)–P(1)′ = 81.25 (6), Cl(1)–Mo(1)–P(1)′ = 165.39 (6)°) in **1** are within expected ranges.

$Mo_2Cl_6(dedppe)_2 \cdot 2CH_2Cl_2$ (**2**) forms monoclinic crystals in the space group $P2_1/c$ with $Z = 2$. The binuclear unit resides on a crystallographic inversion center. As can be clearly seen from the drawing in Figure 2, molecules of **2** bear a close resemblance to those of compound **1**. The two unsymmetrical dedppe phosphines occupy equatorial positions with the ethyl groups on opposite sides of the molecule. The Mo(1)–Mo(1)′ distance in **2** is 2.785 (3) Å, slightly longer than in **1**. All other aspects of the two structures including interatomic distances and angles are very similar. There are the expected, slight differences between the Mo–PEt_2– and Mo–PPh_2– bond lengths, with the latter being longer by 0.017 (9) Å, which is, of course, barely significant in a statistical sense.

A third compound, $W_2Cl_6(dppe)_2 \cdot 4CH_2Cl_2$ (**3**), which is the tungsten homologue of **1**, forms triclinic crystals ($P\bar{1}$) with $Z = 2$. The asymmetric unit consists of two independent molecules of $W_2Cl_6(dppe)_2$. The distances and angles within the two unrelated dimers are identical within experimental error. An ORTEP diagram of the molecule is shown in Figure 3. Some average distances are W–Cl_b = 2.402 [3], W–Cl_t = 2.394 [4], and W–P = 2.529 [4] Å, which are all slightly shorter than the corresponding values in $Mo_2Cl_6(dppe)_2$. The nonlinear angle Cl_t–W–Cl_t of 163.6 [1]° and the angles between the tungsten atoms and chlorine bridges (W–Cl_b–W(av) = 67.88 [9], Cl_b–W–Cl_b = 112.1 [1]°) are indicative of a strong M–M interaction. The average W–W distance in $W_2Cl_6(dppe)_2$ is 2.681 [1] Å, shorter by ~0.08 Å than the Mo–Mo distance in $Mo_2Cl_6(dppe)_2$.

Table VII. Selected Bond Distances (Å) and Angles (deg) and Their Estimated Standard Deviations for $W_2Cl_6(dppe)_2 \cdot 4CH_2Cl_2$ (**3**)[a]

Distances			
W(1)′–W(1)	2.682 (1)	W(2)–Cl(5)	2.387 (4)
W(1)–Cl(1)	2.391 (3)	W(2)–Cl(6)	2.401 (3)
W(1)–Cl(2)	2.397 (4)	W(2)–P(3)	2.526 (4)
W(1)–Cl(3)	2.404 (3)	W(2)–P(4)	2.529 (3)
W(1)–P(1)	2.528 (3)	P(1)–C(1)	1.826 (15)
W(1)–P(2)	2.533 (4)	P(1)–C(13)	1.859 (14)
W(2)′–W(2)	2.680 (1)	P(2)–C(14)	1.834 (14)
W(2)–Cl(4)	2.401 (4)	P(4)–C(40)	1.865 (13)
Angles			
W(1)′–W(1)–Cl(1)	97.77 (8)	W(2)′–W(2)–P(4)	138.07 (9)
W(1)′–W(1)–Cl(2)	97.89 (7)	Cl(4)–W(2)–Cl(5)	163.0 (1)
W(1)′–W(1)–Cl(3)	56.00 (6)	Cl(4)–W(2)–Cl(6)	92.1 (1)
W(1)′–W(1)–P(1)	139.66 (9)	Cl(4)–W(2)–P(3)	81.9 (1)
W(1)′–W(1)–P(2)	138.34 (7)	Cl(4)–W(2)–P(4)	83.9 (1)
Cl(1)–W(1)–Cl(2)	164.2 (1)	Cl(5)–W(2)–Cl(6)	98.2 (1)
Cl(1)–W(1)–Cl(3)	96.0 (1)	Cl(5)–W(2)–P(3)	84.6 (1)
Cl(1)–W(1)–P(1)	83.4 (1)	Cl(5)–W(2)–P(4)	84.2 (1)
Cl(1)–W(1)–P(2)	84.8 (1)	Cl(6)′–W(2)–Cl(6)	112.1 (1)
Cl(2)–W(1)–Cl(3)	91.3 (1)	Cl(6)–W(2)–P(3)	163.7 (1)
Cl(2)–W(1)–P(1)	83.6 (1)	Cl(6)–W(2)–P(4)	82.1 (1)
Cl(2)–W(1)–P(2)	84.6 (1)	P(3)–W(2)–P(4)	82.1 (1)
Cl(3)′–W(1)–Cl(3)	112.1 (1)	W(1)–Cl(3)–W(1)	67.87 (9)
Cl(3)–W(1)–P(1)	83.7 (1)	W(2)–Cl(6)–W(2)	67.90 (9)
Cl(3)–W(1)–P(2)	165.5 (1)	W(1)–P(1)–C(1)	122.3 (5)
P(1)–W(1)–P(2)	82.0 (1)	W(1)–P(1)–C(13)	106.5 (4)
W(2)′–W(2)–Cl(4)	98.46 (7)	W(1)–P(2)–C(14)	105.4 (6)
W(2)′–W(2)–Cl(5)	98.46 (7)	W(2)–P(4)–C(40)	106.8 (4)
W(2)′–W(2)–Cl(6)	56.00 (7)	P(1)–C(13)–C(14)	110.0 (8)
W(2)′–W(2)–P(3)	139.77 (7)		

Table VIII. Parameters from the Best Fit of Eq 1 to the Magnetic Data for **1** and **3**

complex	g	$E(^3B_{1u})$, cm^{-1}	$E(^1B_{1u})$, cm^{-1}	TIP, emu/mol	% impurity
$Mo_2Cl_6(dppe)_2$ (**1**)	1.99	941	1600	0.000 24	0.017
$W_2Cl_6(dppe)_2$ (**3**)	1.99	1115	2200	0.000 035	0.03

Magnetic Behavior. Figure 4 illustrates the qualitative orbital and state energy level diagrams for metal–metal bonding through edge-sharing octahedra. The magnetic behavior of the binuclear molecules is determined by the extent of population of the excited paramagnetic ($^3B_{1u}$) state relative to the singlet states. Although we have assumed the δ orbital to be lower in energy [$E(\delta) < E(\delta^*)$)], the order of splitting of the states is the same for the case where $E(\delta^*) < E(\delta)$.

The magnetic susceptibility that arises from a molecule that has energy levels corresponding to the diagram shown in Figure 4, may be derived using the Van Vleck formula[19] and is given in the following closed-form equation

$$\chi = \frac{Ng^2\mu_B^2}{kT} \frac{2e^{-x_1}}{1 + 3e^{-x_1} + e^{-x_2} + e^{-x_3}} \quad (1)$$

where $x_1 = E(^3B_{1u})/kT$, $x_2 = E(^1B_{1u})/kT$, and $x_3 = E(^1A_{1g}^*)/kT$ and all of the other parameters have their usual meaning. Magnetic susceptibility data for compounds **1** and **3** are shown in Figures 5 and 6. The solid lines drawn through the data points are the best fits of the above equation to the magnetic data, including corrections for temperature-independent paramagnetism (TIP) and a paramagnetic impurity assumed to be a Mo(III) monomer with $S = {}^3/_2$. The fitted parameters are listed in Table VIII.

Because the singlet excited states cause only a small modification of the high-temperature magnetism, the quality of the fit was insensitive to variation of these values and a wide range of values for $E(^1B_{1u})$ and $E(^1A_{1g}^*)$ gave equally acceptable fits. The energies of $E(^1B_{1u})$ and $E(^1A_{1g}^*)$ were constrained so that $E(^1A_{1g}^*) = 2E(^1B_{1u})$. Even with this constraint, the fitting was relatively insensitive to variations in the singlet energies, especially as the $E(^3B_{1u})$ value increased above 1000 cm^{-1}.

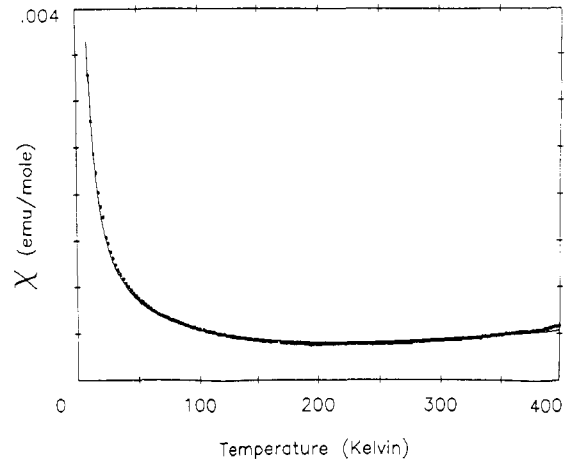

Figure 5. Plot of molar magnetic susceptibility vs temperature for **1**. Points are experimental and the line is from eq 1 with the parameters listed in Table VIII.

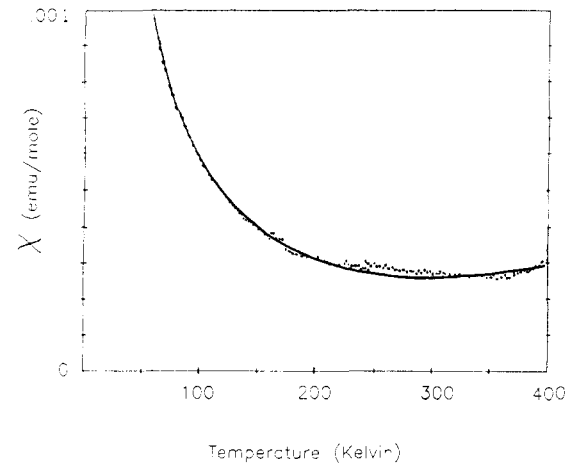

Figure 6. Plot of molar magnetic susceptibility vs temperature for **3**. Points are experimental and the line is from eq 1 with the parameters listed in Table VIII.

The quality of the fit was very sensitive to the value of $E(^3B_{1u})$ and therefore the value of the triplet $\delta\delta^*$ energy is relatively accurate. However, the uncertainty in this parameter increases as the magnitude of the $E(^3B_{1u})$ energy increases.

Complexes **1** and **3** do not exhibit temperature-dependent magnetic properties consistent with thermal population of an accessible excited triplet state. The energies of the $^3B_{1u}$ state for $M_2Cl_6(dppe)_2$ (M = Mo, W) are 941 and 1115 cm^{-1}, respectively. The values of $E(^3B_{1u})$ are between 600 and 800 cm^{-1} for the μ-thiolate compounds with chelating dithiadecane or dithiaoctane ligands.[6] On the other hand, a study of the μ-SEt compound $Mo_2(\mu\text{-}SEt)_2Cl_4(dmpe)_2$[6] possessing chelating phosphines revealed essentially diamagnetic behavior with $E(^3B_{1u}) = 1077$. These results suggest that the M–M bonding in the $(L\text{–}L)Cl_2M(\mu\text{-}X)_2MCl_2(L\text{–}L)$ compounds is influenced by the nature of the donor atoms L in the equatorial positions to an even greater degree than by the identity of the bridging group X^- (SR vs Cl).

Metal–Metal Bonding. The question of how the d^3–d^3 configurations interact with one another is a major topic of interest in the study of Mo_2^{6+} and W_2^{6+} complexes. We discussed this point in detail in the earlier paper[6] where our conclusion, based upon theoretical and structural data, was that the effective Mo–Mo bond order in $Mo_2(\mu\text{-}SR)_2Cl_4(L\text{–}L)_2$ compounds is 2. The double-bond interpretation arises from the fact that σ and π levels are doubly occupied and the δ and δ^* levels are practically nonbonding.

Calculations were not carried out for the present study, but the structural similarity, including M–M distances in the range 2.68–2.78, of the new compounds to those previously reported suggest a M=M double bond.

Electronic Spectroscopy and Electrochemistry. $Mo_2Cl_6(dppe)_2$ was studied by UV–visible spectroscopy in CH_2Cl_2 solution. Characteristic spectral features are as follows (λ_{max}, nm (ϵ)): 232 (122 000), 310 (7200), 392 (380), and 507 (2050).

A cyclic voltammogram of **1** in 0.2 M TBAH in CH_2Cl_2, available as supplementary material, revealed one irreversible reduction wave at $E_{1/2} = -1.10$ V and two reversible one-electron oxidations at $E_{1/2} = +1.45$ V and $E_{1/2} = +0.85$ V vs Ag/AgCl. For these couples, the $i_{p,a}/i_{p,c}$ ratios were close to unity and the separation (ΔE_p) between the anodic and cathodic peaks was ~65 mV at a scan rate of 200 mV/s. The oxidations correspond to the processes $Mo^{III}Mo^{III} - e^- \rightarrow Mo^{III}Mo^{IV}$ and $Mo^{III}Mo^{IV} - e^- \rightarrow Mo^{IV}Mo^{IV}$.

In contrast to the above redox chemistry, the cyclic voltammogram of the quadruply bonded β-$Mo_2Cl_4(dppe)_2$[22] consists of only one accessible oxidation ($Mo^{II}Mo^{II} - e^- \rightarrow Mo^{II}Mo^{III}$), attesting to the stability of the $\sigma^2\pi^4\delta^2$ configuration.

Concluding Remarks. We have demonstrated that the quadruple bonds of dimolybdenum and ditungsten undergo facile oxidative addition reactions with Cl_2. The reactions can be controlled to produce the desired M_2^{6+} compounds in high yield.

The isolation and structural characterization of the complexes $Mo_2Cl_6(dedppe)_2$ and $M_2Cl_6(dppe)_2$ (M = Mo, W) increases our gallery of M_2L_{10} compounds possessing an edge-sharing bioctahedral geometry. The dppe compounds are particularly interesting because they belong to a homologous series that now includes examples with the metals Zr, Nb, Ta, Mo, W, and Re. We hope to be able to prepare the Tc, Ru, and Os analogues as well.

One interesting aspect of the structures reported here is that the $M_2Cl_6(dppe)_2$ molecules, in which the diphosphine ligands could not be supposed to play any role in tying the metal atoms together, have approximately the same M–M distances as those found in the $M_2Cl_6(dppm)_2$ molecules,[23] where such a role might be postulated. Thus, we have the following comparisons of M–M distances, in Å:

$Mo_2Cl_6(dppm)_2$	2.789 (1)	$Mo_2Cl_6(dppe)_2$	2.762 (1)
$W_2Cl_6(dppm)_2$	2.691 (1)	$W_2Cl_6(dppe)_2$	2.682 (1)

In fact, to the extent that differences exist between dppm and dppe compounds with the same metal atom, it is the former which have the longer M–M bonds.

Another notable point is that the tendency of the W–W bonds to be ca. 0.10 Å shorter than analogous Mo–Mo bonds seems to be independent of the exact arrangement of the ligands, that is, whether the diphosphines bridge axial positions or chelate in the equatorial plane.

Acknowledgment. We thank the National Science Foundation for support.

Registry No. **1**, 110900-34-0; **2**, 110717-87-8; **3**, 110717-89-0; $Mo_2Cl_6(dppe)_2$, 92479-08-8; $W_2Cl_6(dppe)_2$, 110717-88-9; β-$Mo_2Cl_4(dppe)_2$, 64508-32-3; α-$Mo_2Cl_4(dppe)_2$, 64490-77-3; $Mo_2Cl_4(dedppe)_2$, 110373-57-4; α-$W_2Cl_4(dppe)_2$, 86782-93-6; β-$W_2Cl_4(dppe)_2$, 73133-24-1; $Mo_2Cl_6(dppe)_2^+$, 110717-90-3; $Mo_2Cl_6(dppe)_2^{2+}$, 110717-91-4; CH_2Cl_2, 75-09-2; Mo, 7439-98-7; W, 7440-33-7; chlorine, 7782-50-5.

Supplementary Material Available: A listing of positional parameters for phenyl group atoms in **3** (Table IVS), full listings of bond angles, bond distances, and anisotropic displacement parameters for **1**–**3**, listings of molar magnetic susceptibility data for **1** and **3**, and a figure depicting the cyclic voltammogram of **3** (22 pages); tables of observed and calculated structure factors for **1**–**3** (50 pages). Ordering information is given on any current masthead page.

(22) Zietlow, T. C.; Klendworth, D. D.; Nimry, T.; Salmon, D. J.; Walton, R. A. *Inorg. Chem.* **1981**, *20*, 947.

(23) Canich, J. M.; Cotton, F. A.; Daniels, L. M.; Lewis, D. B. *Inorg. Chem.*, in press.

Contribution from the School of Chemistry,
University of New South Wales, Kensington, NSW 2033, Australia

The Different Nonmolecular Polyadamantanoid Crystal Structures of $Cd(SPh)_2$ and $Cd(SC_6H_4Me\text{-}4)_2$. Analogies with Microporous Aluminosilicate Frameworks[1]

Ian G. Dance,* Robert G. Garbutt, Donald C. Craig, and Marcia L. Scudder

Received March 3, 1987

$Cd(SPh)_2$ (**2**) crystallizes unsolvated from DMF with a structure (orthorhombic, $P2_12_12_1$, $a = 15.490$ (2) Å, $b = 15.626$ (2) Å, $c = 20.803$ (3) Å, $Z = 16$ ($CdS_2C_{12}H_{10}$), 3626 observed data, Mo Kα, $R = 0.034$) in which adamantanoid cages comprised of four Cd atoms and six doubly bridging SPh ligands are connected in three dimensions by doubly bridging SPh ligands. The lattice arrangement of the linked tetrahedral adamantanoid cages is almost identical with that of the α-cristobalite form of SiO_2. The structure of crystalline $Cd(SC_6H_4Me\text{-}4)_2$ (**3**) (monoclinic, $P2_1/c$, $a = 27.196$ (9) Å, $b = 15.722$ (5) Å, $c = 37.046$ (13) Å, $\beta = 132.03$ (1)°, $Z = 32$ ($CdS_2C_{14}H_{14}$), 12 003 observed data with $(\sin\theta)/\lambda > 0.1$ Å^{-1}, Mo Kα, $R = 0.065$) is also three-dimensionally nonmolecular with vertex-linked adamantanoid tetrahedra, but in a very different linkage pattern involving closed four-, six-, and eight-membered rings of tetrahedra, resembling microporous zeolite lattices. In **3** there exist very large centrosymmetric cavities in the Cd,S array, surrounded by 12 adamantanoid cages whose centroids constitute a trans truncated octahedron. Channels encycled by eight-membered rings also exist in the lattice. The cavities are lined with 44 S atoms connected by 32 Cd atoms, contain 10 ligand substituents, and are connected through four- and six-membered rings to other cavities. Within the cavities the S---S diagonals through the inversion center range from 16.6 to 19.1 Å. The volumes excluded by the Cd,S cores of the adamantanoid tetrahedra are 12% and 10% of the unit cell volumes in **2** and **3**, respectively, and the remaining volumes occupied by the substituents are partially empty. Both of these poly-linked-adamantanoid structures are unique.

Introduction

Although the chemistry of anionic polymetallic thiolate complexes $[M_x(SR)_y]^{z-}$ has been developed quite extensively, at least for some metals, fundamental knowledge of the structures of the uncharged metal thiolates $[M(SR)_n]_p$ is relatively sparse.[2] This is due in part to the relative insolubility of the uncharged compounds in inert solvents, attributed to structural nonmolecularity in the crystal phase, and the consequent problem of obtaining crystals of diffraction quality.

We are concerned here with the structural chemistry of the set of compounds $M(SR)_2$ (R noncoordinating) in which M is tet-

(1) Previous paper in this series on polycadmium complexes: Dance, I. G.; Garbutt, R.; Craig, D. C. *Inorg. Chem.* **1987**, *26*, 3732.

(2) Dance, I. G. *Polyhedron* **1986**, *5*, 1037.

0020-1669/87/1326-4057$01.50/0